

E. PALACIOS-LIDÓN¹
H.M. YATES²
M.E. PEMBLE²
C. LÓPEZ¹,✉

Photonic band gap properties of GaP opals with a new topology

¹Instituto de Ciencia de Materiales de Madrid (CSIC) C/Sor Juana Inés de la Cruz 3, 28049 Madrid, Spain

²Institute of Materials, Cockcroft Building, University of Salford, Salford, M5 4WT, UK

Received: 18 January 2005

Published online: 15 July 2005 • © Springer-Verlag 2005

ABSTRACT In this paper, we propose that the “anomalous” optical response exhibited by GaP and InP infiltrated opals is due to the peculiar morphology shown by these materials when grown within the pores. In order to account for their optical response, we propose a new structural model consisting of a network of high dielectric spheres located in the pores of the bare opal, interconnected by cylinders of the same material. A fair agreement between the theoretical predictions using this model and the experimental measurements has been found. We also show that the inverse structure presents very interesting optical properties.

PACS 42.70.Qs; 42.25.Fx; 42.25.Gy

1 Introduction

The study of synthetic opals as photonic crystals (PC) has been a topic of increasing interest in the last few years [1]. These materials are prepared from colloidal systems in which silica or polymer spherical particles settle down into a closed-packed face centre cubic (fcc) lattice. PCs exhibit a periodic modulation in the refractive index and, consequently, peculiar properties for photon propagation are expected [2, 3]. By filling the interparticle voids with different materials, it is possible to obtain structures apt to be used as sensors [4], photonic inks [5], etc. When the infiltrated material has a high enough refractive index ($n > 2.8$), and after the removal of the spheres' matrix, the resulting inverse opal shows stop bands for all directions of photon propagation [6, 7] known as full photonic band gaps (PBG). Up to now, inverse opals of semiconductors, such as Silicon [8] and Germanium [9], presenting a PBG have been obtained. However, the presence of very high absorption in the infrared range becomes an issue in their use as devices working in the visible range.

A fine solution to this problem is the infiltration of opals with certain III–V compounds. These materials have high refractive index and are transparent in the visible range (GaP) or near infrared (InP, GaAs) [10]. Additionally, these materials are very important in many technological fields because they

present interesting properties, such as luminescence [11] non-linear optics effects [12], etc., that make them suitable in many device applications. A periodic macroporous network formed with one of these materials would offer the possibility of coupling the photonic and electronic properties. However, infilling with these type of compounds is a difficult task and (in fact, only a few inverse opals have been demonstrated) more so with III-nitrides [13]. Lee et al. [14] reported the preparation of a Gallium Arsenide (GaAs) inverse opal infilled by electrochemical deposition, although they concluded that there was little chance of obtaining other III–V materials, such as GaP or InP using this method.

Recently, we showed for the first time the possibility of Indium Phosphide (InP) or Gallium Phosphide (GaP) opals infiltration by using a Metal-organic Chemical Vapour Deposition (MOCVD) method [15]. Although X-ray diffraction and Raman studies revealed they are crystalline III–V materials of very good quality, their optical response (Fig. 1) could not be explained by the usual infiltration model termed surface templating [16]. In such a model the infiltrated material is assumed to grow uniformly around the opal spheres making shells of increasing thickness. As the infiltration progresses the shell radius gets larger and larger until, eventually, the inter-sphere voids become filled. This behaviour has been reported in many studies using materials, such as Si [17], Ge [18], and SiO₂ [19] for instance.

2 III–V infiltration

According to this model, as the infilling degree increases the Bragg peak, corresponding to the first pseudogap in the (1 1 1) direction, shifts toward higher wavelengths. If the infilled material has a refractive index $n > 3$, this shift may amount to a few hundred nanometres [8]. At the same time the width of this Bragg peak dramatically increases. GaP infiltrated opals present, however, a very different behaviour, as can be seen in Fig. 1. Surprisingly, the reflectance spectra show a Bragg peak with no appreciable shifting with reference to the bare opal. According to the above model, this would mean that all studied samples would have a negligible filling fraction. The appearance of intense high-energy peaks in the reflectance spectra is in clear contradiction with the assumption of a low degree of infiltration. Another important fact to be highlighted is that (apart from small differences caused

✉ Fax: +34 91 334 9019, E-mail: cefe@icmm.csic.es
Present address: NMRC, Lee Maltings, Prospect Row, Cork, Ireland

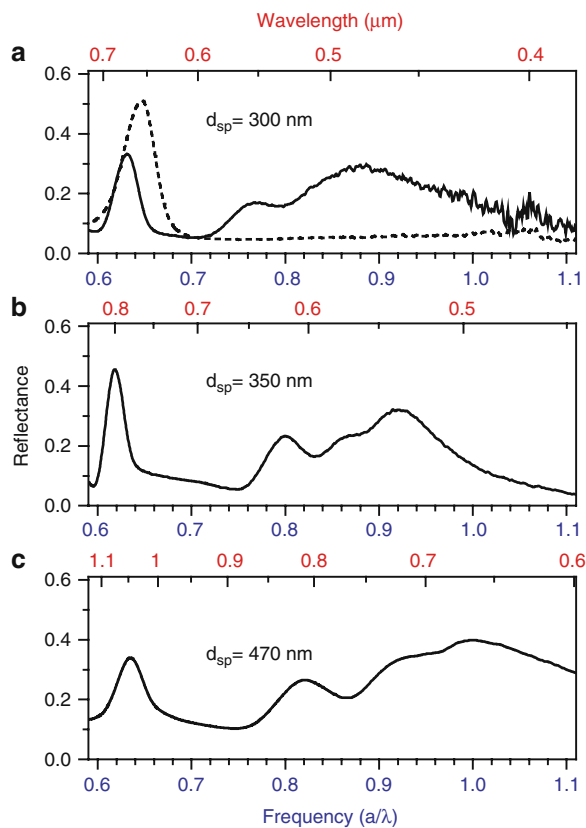


FIGURE 1 Reflectance spectra of GaP infiltrated opals for three different sphere sizes (*solid lines*) **a** 300 nm **b** 350 nm **c** 470 nm. In **a** the spectrum of the bare opal (*dash line*) has also been included for comparison showing there is no substantial shift with respect to the infiltrated one. Note the top axes in the three plots showing that the same features appear in different absolute ranges depending on the sphere size

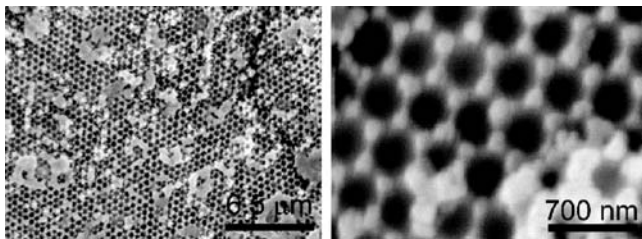


FIGURE 2 SEM photographs of inverse GaP opals ($d_{sp} = 350$ nm). From these micrographs a lattice parameter $a = 528$ nm can be derived which is 33 nm larger than that of the original opal, in agreement with the required lattice expansion

by little changes in infiltration degree and chromatic dispersion of GaP) all spectra show similar overall appearances in reduced units (a/λ). These findings confirm that all of the studied samples exhibit a reproducible photonic behaviour, i.e., it is scalable with the lattice parameter. However, the strongest evidence for the failure of the surface templating model predictions for this particular case is gained from SEM characterization (Fig. 2) and the actual possibility of obtaining inverted opals: high amounts of GaP are available to build up a framework which is stable after the spheres template is removed.

A recent study conducted on InP grown opals shows that when the infiltration degree is high, the infiltrated material tends to grow as large grains filling the interspherical voids

instead of forming uniform coatings [15]. This produces an abrupt change in the optical response similar to that exhibited by the GaP opals. This is to be expected since GaP and InP are very similar materials prepared with related precursors under similar growth conditions. A detailed inspection of the magnified SEM picture (Fig. 2b) of the GaP inverse opal evidences a structure in which large spherical grains of GaP mostly filling the voids appear connected through thin necks. Given the important role of these materials for optoelectronics applications it becomes a pressing necessity to cast light on these apparent contradictions and find an explanation to the photonic band gap behaviour of GaP composite and inverted opals.

3 Model

In this paper, we propose that the “anomalous” optical response exhibited by GaP and InP infiltrated opals is due to the peculiar morphology shown by these materials when grown within the pores. In order to account for their optical response, we propose a new structural model consisting of a network of high dielectric spheres located in the pores of the bare opal, interconnected by cylinders of the same material. A fair agreement between the theoretical predictions using this model and the experimental measurements has been found. In addition, we also show that the inverse structure presents very interesting optical properties.

In a close packed fcc crystal (see Fig. 3), there are two different sets of pores between nearest spheres of diameter d_{sp} : large voids of diameter $d_1 = 0.41d_{sp}$ and small voids of diameter $d_2 = 0.23d_{sp}$. These voids form a CaF₂ lattice [16] with large voids located at the Ca position (octahedral coordination) and small pores at the F position (tetrahedral coordination). These pores are connected through bottleneck constrictions. The minimum diameter of this constriction is given by $d_{cyl} = 2 \times 3^{-1/2}D - d_{sp}$, where D is the distance between nearest spheres [16]. In a closed packed structure ($D = d_{sp}$) this becomes $d_{cyl} = 0.15d_{sp}$. From SEM images (Fig. 2b), it can be seen that there are no apparent differences in size between the spheres located at large and small

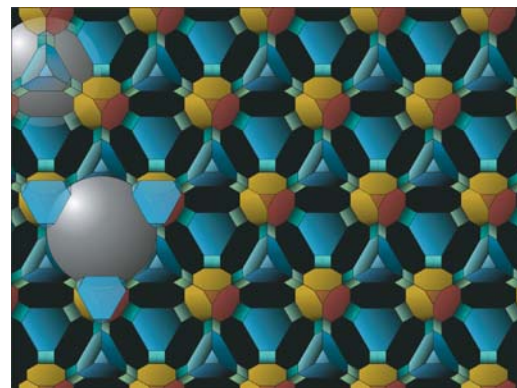


FIGURE 3 Structure of pores in an artificial opal comprising tetrahedral voids (*blue*) bounded by four spheres and octahedral ones (*brown*) bounded by six spheres. Two spheres from the opal are also drawn which belong to two different layers. The pores are connected by triangular prisms bounded by three spheres. In the model pores have been represented either by spheres or cylinders (*colour online*)

pores. Furthermore, these are larger than their expected small size according to the corresponding voids. This fact implies a structure expansion that increases the lattice parameter by an amount of $2 \times 3^{-1/2} \Delta d_2$ without altering the fcc symmetry. This is possible if we assume that all grains grow at the same rate during the CVD growth process and the supporting matrix can be expanded without any mechanical resistance (which is the case as the opal is not sintered). Similar lattice changes have been reported for infiltrated materials prepared by other methods [20].

The band calculations have been done using the MPB package [21], developed at MIT based on an iterative plane wave expansion method. Our proposed model for infiltrated GaP consists of an fcc lattice of silica spheres (bare opal) where spheres of higher dielectric material (GaP) fill the voids (Fig. 4a). The connections between these spheres have been modelled with cylinders. If all spheres are assumed to be of the same size (Fig. 4b) and located in the pores, it is necessary to consider the lattice expansion mentioned above keeping in mind that the silica matrix would not be closed-packed

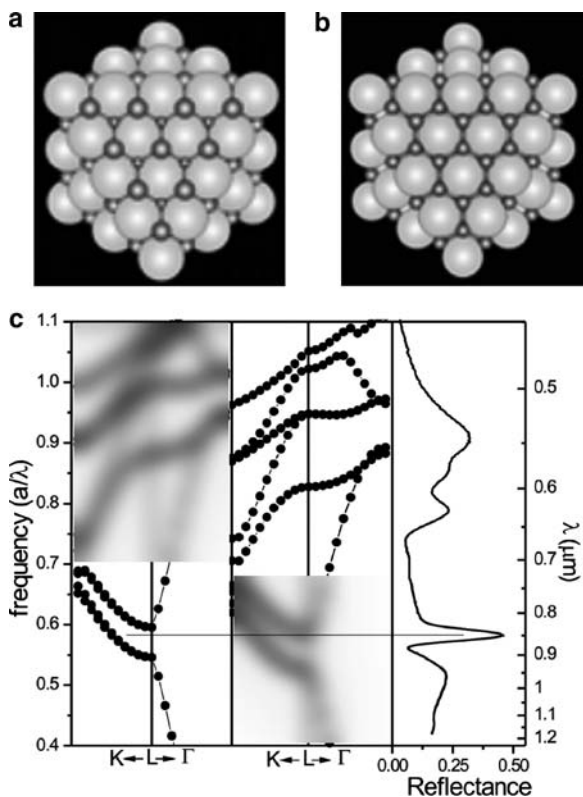


FIGURE 4 The proposed structure can be described as an fcc lattice with a silica sphere situated at the origin and a basis made of one large pore in $(0, 0, \frac{1}{2})$ and two small pores at $(\frac{1}{4}, \frac{1}{4}, \frac{1}{4})$ and $(-\frac{1}{4}, -\frac{1}{4}, -\frac{1}{4})$. In order to include the connections between large and small pores, four different cylinders centred at the large pore position were added. **a** Closed-packed fcc lattice of silica spheres; the size of the spheres situated in the large and small voids are clearly different. **b** Same structure as **a** but with $d_1 = d_2 = 0.11a$, the expansion of the lattice (explained in the text is evident) **c** Comparison between theoretical predictions and experimental results. The calculation parameters where $d_1 = d_2 = 0.22a$ and $d_{cyl} = 0.11a$, mesh = 7 and $N_g = 32$. Taking into account the GaP chromatic dispersion in the working wavelength range, we chose $\epsilon = 9.61$ for the low energy bands (1st–5th) and $\epsilon = 11.56$ for the high energy bands (5th–9th). All the bands have been included in both graphs to appreciate the strong dependence of the band energy position with the refractive index. The bands that are not compared have been blurred

any more. Additionally, if a comparison between theoretical predictions of the structural model and experimental results is desired, it is also worthwhile noticing that the GaP has a strong chromatic dispersion [22] in the wavelength range of interest, in which its refractive index varies between 3.15 at 800 nm and 3.45 at 500 nm.

4 Results

Comparison between the reflectance spectrum of the GaP infilled opal with the calculated band structure using the proposed model is shown in Fig. 4c and the observed agreement is fairly good. Calculations have been done using a refractive index $n = 3.1$ for low energy bands (bands 1st–4th) and $n = 3.4$ for the high energy region (bands 5th–9th). Starting with an approximated parameter taken directly from SEM images, the best agreement was found assuming $d_1 = d_2 = 0.22a$ and $d_{cyl} = 0.11a$ where a is the lattice parameter. It was found that small variations in the structural parameters (spheres and cylinder radius) used for calculations do not affect the calculated band structure substantially, only small shifts in the pseudogaps position are observed.

By removing the silica spheres using chemical etching, the inverse structure of GaP is achieved. The inset to Fig. 5a shows a representation of the resulting crystal. The band structure of this inverse structure (Fig. 5a) can be easily obtained just by substituting the silica spheres with air spheres in the previously commented upon composite calculations. The refractive index of GaP has been taken as $n = 3.4$ because the most interesting applications of this systems would be near the optical absorption edge (550 nm) of the semiconductor.

Although this structure has not a complete PBG, a pronounced broad pseudogap is apparent between the 5th and 6th bands. This fact is confirmed in experimental measurements finding an intense reflectance peak at the expected frequencies. The presence of a sharp deep can be associated with the presence of flat bands that act as defects embedded in a wider gap.

The proposed structural model is similar to that previously reported by Dong et al. [23] and referred to as a “skeleton” and, although no optical characterization was shown there, a similar optical behaviour is expected. If some of the structural parameters are judiciously varied, the pseudogap becomes a PBG. The evolution of the PBG between the 5th and 6th bands depends on the GaP sphere and cylinder radii as shown in Fig. 6. The PBG opening is mostly determined by the cylinder radius that should reach a threshold value of $0.055a$. Broadening increases with cylinder size. If the cylinder radius is fixed and the sphere radius is taken as parameter, a broader PBG is found not at the largest sphere sizes but at an intermediate value.

Experimentally, the structure parameters are strongly determined by those of the template used in the infiltration. In a typical artificial opal, modification of the structure parameters is highly constrained by the small pore size that limits the cylinder radius. For obtaining a cylinder thick enough to open a PBG, it would be necessary to have a large increase of the small pore size and, consequently, a lattice expansion difficult to control. This problem can be solved by using a non closed

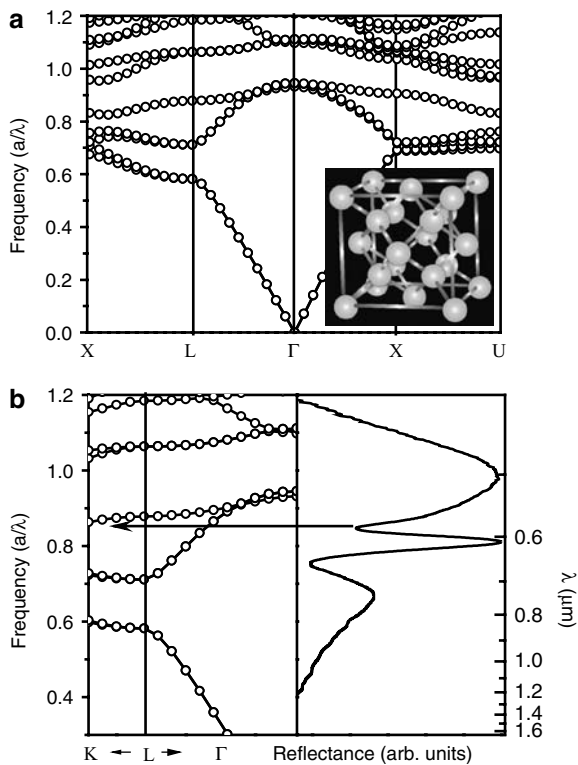


FIGURE 5 **a** Band Structure of the inverse opal using $r_{\text{cyl}} = 0.051$, $r_1 = 0.11$ and $\varepsilon = 11.56$. A broad pseudogap appears between the 5th and 6th bands. Inverse structure lattice. The inset shows the network of filled pores as a ball and stick diagram. The big void spheres correspond to the ones situated at the corners and centres of the faces. The small void spheres are situated in the diagonals of the cube. Both the radii of the cylinders and the spheres ($d_1 = d_2$) have been reduced to have a more open and clear structure. **b** Experimental reflectance spectrum and section of the band structure relevant to the data joined for comparison

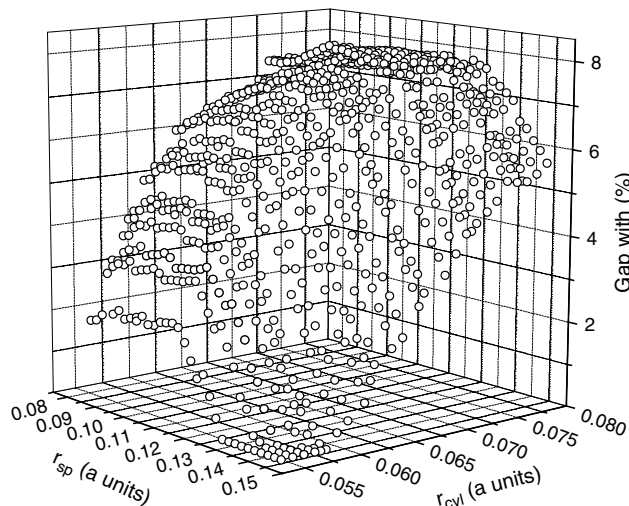


FIGURE 6 Dependence of the width of the PBG between the 5th and 6th bands on the cylinder and pore radii taken

packed artificial opal as template [24] or by regrowing after inversion.

In conclusion, we have contributed to an explanation of the unusual optical behaviour of MOCVD grown InP and GaP infilled opals. Based on the optical behaviour, we have shown that the inverse replicas are grown under a novel structure that can eventually exhibit a PBG between the 5th and 6th bands, by just small modifications in the structure parameters. These can be easily controlled by using an appropriate template for the infiltration. This method of preparation enables real photonic structures of III–V materials to be obtained, which exhibit a PBG in the visible range widening the possibilities for their potential applications as photonic devices. Additionally, this study hopes to stimulate the synthesis of CaF₂-type and other new structures (using opaline templates or otherwise) owing to the PBG properties such lattices develop.

ACKNOWLEDGEMENTS This work is partially financed by the European Commission through IST-1999-19009 PHOBOS project and Spanish MEC through MAT 2003-01237 project. E. P-L thanks Comunidad Autónoma de Madrid for a predoctoral grant.

REFERENCES

- 1 C. López, *Adv. Mater.* **15**, 1679 (2003)
- 2 E. Yablonovitch, *Phys. Rev. Lett.* **58**, 2059 (1987)
- 3 S. John, *Phys. Rev. Lett.* **58**, 2486 (1987)
- 4 S.A. Asher, A.C. Sharma, A.V. Gaponenko, M.M. Ward, *Anal. Chem.* **75**, 1676 (2003)
- 5 A. Arsenault, H. Míguez, V. Kitaev, I. Manners, G. Ozin, *Adv. Mater.* **15**, 503 (2003)
- 6 H.S. Sözüer, J.W. Haus, R. Inguva, *Phys. Rev. B* **45**, 13962 (1992)
- 7 K. Busch, S. John, *Phys. Rev. E* **58**, 3896 (1998)
- 8 A. Blanco, E. Chomski, S. Grachtak, M. Ibisate, S. John, S.W. Leonard, C. López, F. Meseguer, H. Míguez, J.P. Mondia, G.A. Ozin, O. Toader, H.M. van Driel, *Nature* **405**, 437 (2000)
- 9 H. Míguez, F. Meseguer, C. López, M. Hologado, G. Andreasen, A. Mijsud, V. Fornés, *Langmuir* **16**, 4405 (2000)
- 10 S. Adachi, *J. Appl. Phys.* **66**, 6030 (1989)
- 11 *Pits and Pores: Formation, Properties and Significance for Advanced Luminescent Materials*, ed. by P. Schmuki, D.J. Lockwood, H.S. Isaacs, A. Bsiesy, The Electrochemical Society, Montreal, PV 97-7 (1997)
- 12 F.J.P. Schuurmans, D. Vanmaekelbergh, J. van de Lagemaat, A. Lagendijk, *Science* **284**, 141 (1999)
- 13 G. Gajiev, V.G. Golubev, D.A. Kurdyukov, A.B. Pevtsov, A.V. Selkin, V.V. Travnikov, *Phys. Stat. Sol. (b)* **231**, R7 (2002)
- 14 Y. Lee, T. Kuo, C. Hsu, Y. Su, C. Chen, *Langmuir* **18**, 9942 (2002)
- 15 H.M. Yates, M.E. Pemble, E. Palacios-Lidón, F. García-Santamaría, I. Rodríguez, F. Meseguer, C. López, *Adv. Funct. Mater.* **15**, 411 (2005)
- 16 A.A. Zakhidov, R.H. Baughman, Z. Iqbal, C. Cui, I. Khayrullin, S.O. Dantas, J. Marti, V.G. Ralchenko, *Science* **282**, 897 (1998)
- 17 F. García-Santamaría, M. Ibisate, I. Rodríguez, F. Meseguer, C. López, *Adv. Mater.* **15**, 788 (2003)
- 18 H. Míguez, E. Chomski, F. García-Santamaría, M. Ibisate, S. John, C. López, F. Meseguer, J.P. Mondia, G.A. Ozin, O. Toader, H.M. van Driel, *Adv. Mater.* **13**, 1634 (2001)
- 19 H. Míguez, N. Tetreault, B. Hatton, S.M. Yang, D. Perovic, G.A. Ozin, *Chem. Commun.* **22**, 2736 (2002)
- 20 J.E.G.J. Wijnhoven, L. Bechger, W.L. Vos, *Chem. Mater.* **13**, 4486 (2001)
- 21 S.G. Johnson, J.D. Joannopoulos, *Opt. Express* **8**, 173 (2001)
- 22 D.E. Aspnes, A.A. Studna, *Phys. Rev. B* **27**, 985 (1983)
- 23 W. Dong, H. Bongard, B. Tesche, F. Marlow, *Adv. Mater.* **14**, 1457 (2002)
- 24 R. Fenollosa, F. Meseguer, *Adv. Mater.* **15**, 1282 (2003)